A modular approach for the generation, storage, mixing, and detection of droplet libraries for high throughput screening†‡

Varun Trivedi,[b] Ankur Doshi,[a] G. K. Kurup,[a] E. Ereifej,[b] P. J. Vandevord[b] and Amar S. Basu*[ab]

Received 7th April 2010, Accepted 5th July 2010
DOI: 10.1039/c004768f

The desire to make microfluidic technology more accessible to the biological research community has led to the notion of "modular microfluidics", where users can build a fluidic system using a toolkit of building blocks. This paper applies a modular approach for performing droplet-based screening, including the four integral steps of library generation, storage, mixing, and optical interrogation. Commercially available cross-junctions are used for drop generation, flexible capillary tubing for storage, and tee-junctions for serial mixing. Optical interrogation of the drops is achieved using fiber-optic detection modules which can be incorporated inline at one or more points in the system. Modularity enables the user to hand-assemble systems for functional assays or applications. Three examples are shown: (1) a "mix and read" assay commonly used in high throughput screening (HTS); (2) generation of chemically distinct droplets using microfractionation in droplets (μFD); and (3) *in situ* encapsulation and culture of eukaryotes. Using components with IDs ranging from 150 μm to 1.5 mm, this approach can accommodate drop assays with volumes ranging from 2 nL to 2 μL, and storage densities ranging from 300 to 3000 drops per metre tubing. Generation rates are up to 200 drops per second and merging rates are up to 10 drops per second. The impact of length scale, carrier fluid viscosity, and flow rates on system performance is considered theoretically and illustratively using 2D CFD simulations. Due to its flexibility, the widespread availability of components, and some favorable material properties compared to PDMS, this approach can be a useful part of a researcher's toolkit for prototyping droplet-based assays.

1. Introduction

Droplet-based microfluidics is an elegant and scalable approach for high throughput chemistry and biology. For a review of droplet-based microfluidics, the reader is referred to several excellent articles on the topic.[1–4] Droplet-based assays are particularly well suited for high throughput screening because they can conduct assays in miniscule volumes. In large scale screening campaigns used in pharmaceutical and proteomic research, the bulk of the cost is attributed to reagents and screening libraries.[5] Current microplate technologies (384 and 1536 well plates) operate on 1–10 μL volumes, and there is considerable interest in scaling assays down to nL or pL volumes to reduce the costs of reagents. Droplet systems have proved to be effective for many types of screens, including cell assays,[6–11] ratiometric screening for protein crystallization conditions,[12,13] and the directed evolution of enzymes.[14–16]

Although much progress has been made in recent years, the medical community has been hesitant in adopting microfluidic technology, citing reasons such as added complexity, concerns for biocompatibility, "impedance mismatch" with existing macroscale tools, and the infrastructure required to design and test custom microfluidic chips. The desire to make microfluidics more accessible has led to the notion of "modular microfluidics", where users can build a fluidic system from a toolkit of building blocks. This approach is analogous to the electronics industry where discrete electronics design (breadboards) can often provide a faster time-to-market than ASICs (application specific integrated circuits). The modular microfluidics model has been proposed by several academic reports,[17–20] and is also being introduced in industry by Labsmith (Livermore CA) and other commercial vendors.

The objective of this research effort is to demonstrate a low-cost, modular approach specifically for droplet-based fluidics. While the prior efforts in modular microfluidics have focused on continuous flow (single-phase) assays, the goal of this report is to show that the modular approach works equally well with droplet-based (multiphase) screening systems, and can do so using off-the-shelf components. This paper will evaluate the advantages/disadvantages, discuss technical considerations, and demonstrate several applications.

The Results and discussion section is divided into two parts. The first discusses individual components for multiscale drop generation, storage, merging, and detection. Commercially available capillary tubing and fittings are used to generate droplets, and perform serial mixing of droplets with a target reagent. Also described are inline optical detection modules which can be incorporated in one or more locations in the system to provide optical interrogation. The second part demonstrates how the components can be easily combined to perform useful and common procedures in droplet-based screening. Three examples

[a]*Electrical and Computer Engineering Department, Wayne State University, Detroit, MI, USA. E-mail: abasu@eng.wayne.edu*
[b]*Biomedical Engineering Department, Wayne State University, Detroit, MI, USA*

† Published as part of a special issue dedicated to Emerging Investigators: Guest Editors: Aaron Wheeler and Amy Herr.

‡ Electronic supplementary information (ESI) available: The ESI contains several videos referenced in the text. See DOI: 10.1039/c004768f

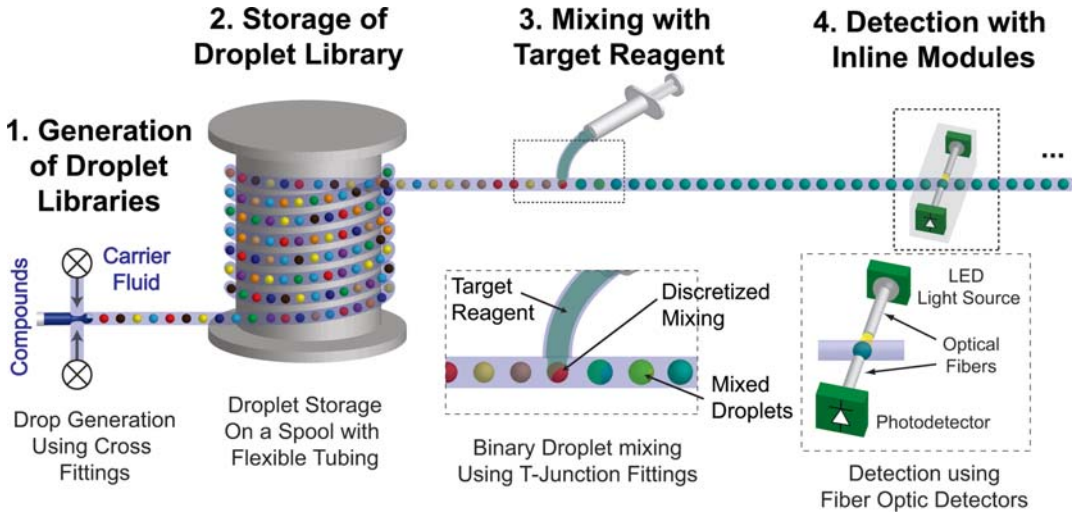

Fig. 1 System concept—a modular approach to droplet-based screening system using off-the-shelf components.

are shown: (1) a "mix and read" assay commonly used in HTS; (2) generation of chemically distinct droplets using microfractionation in droplets (μFD); and (3) *in situ* encapsulation and cell culture. The components and subsystems discussed in this paper can be combined to realize a modular screening system such as the one shown in Fig. 1. In this example, a droplet library is generated by μFD (or other process) and stored in a capillary tube. The library is then serially mixed with a target reagent, and the results are assayed using one or more inline detectors. When required, the droplets can be incubated *in situ* for cell culture.[11]

The use of components familiar to the biological research community may increase the likelihood that this approach will be adopted. The components used are inexpensive (in most cases, disposable), readily available in large quantities, autoclavable, and are composed of materials generally accepted as biologically inert (Teflon, PEEK). Furthermore, the components are available at a wide range of inner diameters (IDs), allowing the user to choose from a wide range of assay volumes.

2. Materials and methods

Fluidic setup

The droplet generation and mixing system utilizes off-the-shelf components as summarized in Table 1. Teflon tubing with 1.5875 (~1.5) mm, 500 μm, and 150 μm inner diameter (ID) were obtained from Upchurch and Small Parts. Cross- and tee-junctions were obtained from Value Plastics, Sigma Aldrich, and Upchurch. For 1.5 mm ID capillaries, plastic cross-connectors with barb type fittings (Fig. 2) provide leak free operation due to low pressures involved. In 500 μm ID and 150 μm ID capillaries, the increased backpressure requires compression fittings. Microbore tee and cross fittings are widely used in high pressure liquid chromatography (HPLC), and are available from

Table 1 Part numbers for fittings used in drop generation and mixing. VP = Value Plastics, SA = Sigma Aldrich, UC = Upchurch

ID	Tubing	Drop generator (cross)	Mixer (tee)	Interconnect to syringe
1.5 mm	SP SWTT-1	VP 4PX210-6	VP T410-6	VP MTLL410-6
500 μm	UC 1548	SA 57663	SA 57661	UC P-659
150 μm	UC P1476	UC P-891	UC P-890	UC P-659

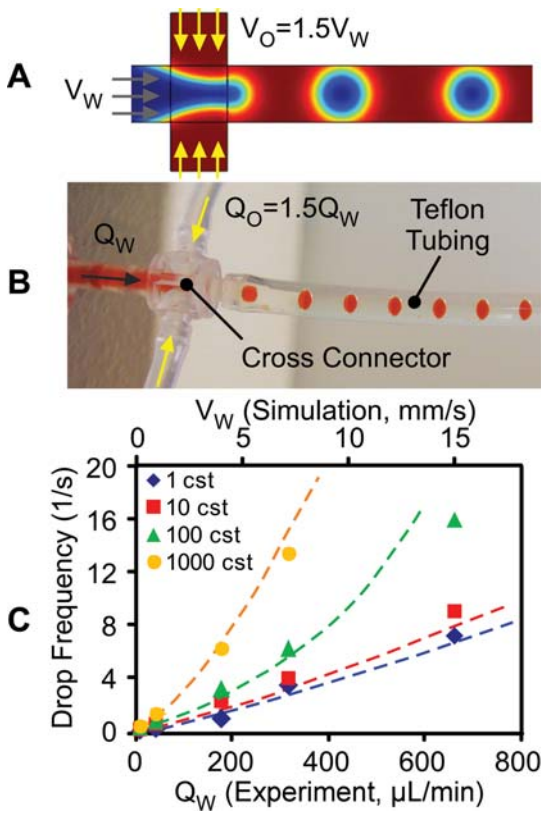

Fig. 2 Simulation and experimental data of an off-the-shelf cross-junction drop generator. (A) CFD simulation, showing velocity of water and carrier fluid. (B) Experimental setup, showing a commercially available 1.5 mm cross-connector and Teflon tubing. (C) Droplet generation rates *versus* flow rate for various viscosities of carrier fluid. Simulation values are shown in dotted lines, and experimental values are shown with data points.

a number of vendors. For interconnect to syringes, plastic luer to barb adapters were used with 1.5 mm ID tubing, and luer to compression adapters were used for smaller capillaries.

The aqueous phase consisted of deionized water with added food dyes (FD&C Red 40, FD&C Blue 1, FD&C Yellow 5) for visualization. The carrier fluid was silicone oil with viscosity 1, 10, 100, and 1000 centistokes (Dow Corning 200 Fluid). The sample and carrier fluid were applied using plastic syringes (BD) driven by a programmable syringe pump (KD Scientific). In all experiments, the water syringe was 5 mL, and the carrier fluid syringe was 10 mL, resulting in a flow rate ratio of carrier fluid to water $Q_O/Q_W \approx 1.48$.

Optical detectors

The fiber optic absorbance detectors (Fig. 3) consisted of an excitation LED coupled into an optical fiber which was orthogonally fixed to the tube carrying the droplets. A second fiber, attached on the opposite end, provided an optical path to the photodetector. The photodetector signal was amplified by a transimpedance amplifier and recorded by a data acquisition card (National Instruments). A custom peak detection algorithm, implemented in Labview (National Instruments), tabulated the amplitude, width, and period of each peak, and recorded relevant statistics (mean, coefficient of variation, histogram). In experiments which measured drop frequencies (Fig. 2 and 4), the sample size ranged from $N = 50$–400 droplets. The peak width, measured in seconds, was correlated to the plug length by multiplying by the flow velocity. The stability of drop generation was quantified using the coefficient of variation (COV). The distribution of droplet sizes was typically Gaussian, and the COV was calculated by dividing the standard deviation of the droplet period by the mean period. LEDs (470 nm, 520 nm, and 650 nm), photodetectors, and polymer optical fiber were obtained from Industrial Fiber Optics (Tempe AZ), and electronic components were obtained from Newark. For the 1.5 mm and 500 μm detectors, optical fibers were stripped of their jackets and epoxied to two opposite ports in a cross connector (Fig. 3B). In the 150 μm detector, two 500 μm optical fibers were placed perpendicular to the capillary using an aluminium housing with alignment grooves (Fig. 3C). To increase light coupling, the fibers were "pigtailed" to the LED by inserting the fiber into a 1 mm diameter hole drilled into the epoxy lens of the LED. Placing the fiber in close proximity to the semiconductor chip increased light coupling by 3–8 fold.

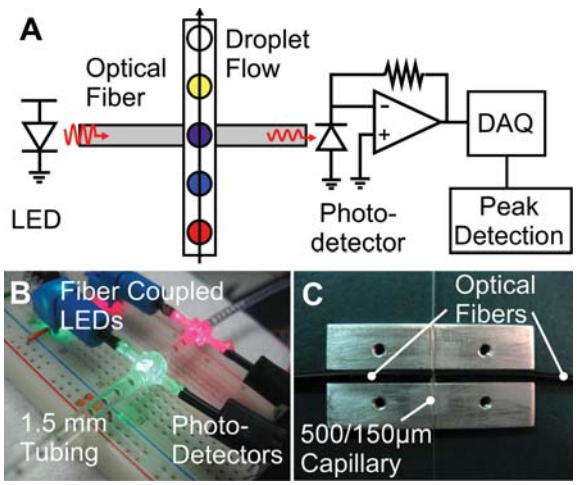

Fig. 3 (A) Schematic of fiber optic absorbance detector. (B and C) Detectors for 1.5 mm, 500 μm and 150 μm capillaries.

CFD simulation

To gain insight and illustrate droplet formation, mixing, and stability, computational fluid dynamics (CFD) simulations were performed using COMSOL Multiphysics (COMSOL). A two-dimensional model was chosen to reduce complexity and computation time. To model the two phases, the level set method was used. Channel geometries were meshed using the free meshing tool, and refined as necessary. Contact angles of the walls were chosen to model the hydrophobicity of the channel wall. The ratio of water to oil velocity was kept at 2 : 3 (since there are two oil inlets, this results in a 1 : 3 ratio of water to carrier fluid). In all simulations, the interfacial tension between the carrier fluid and water was set to 30 mN m^{-1}, chosen based on previous literature which reports the interfacial tension of water/silicone oil to be between 28 and 35 mN m^{-1}.[21,22] Surfactants such as Span 80 can bring the interfacial tension down to 3 mN m^{-1},[23] and interfacial tension can vary from 3–18 mN m^{-1} depending on the temperature difference between the two phases. In this effort,

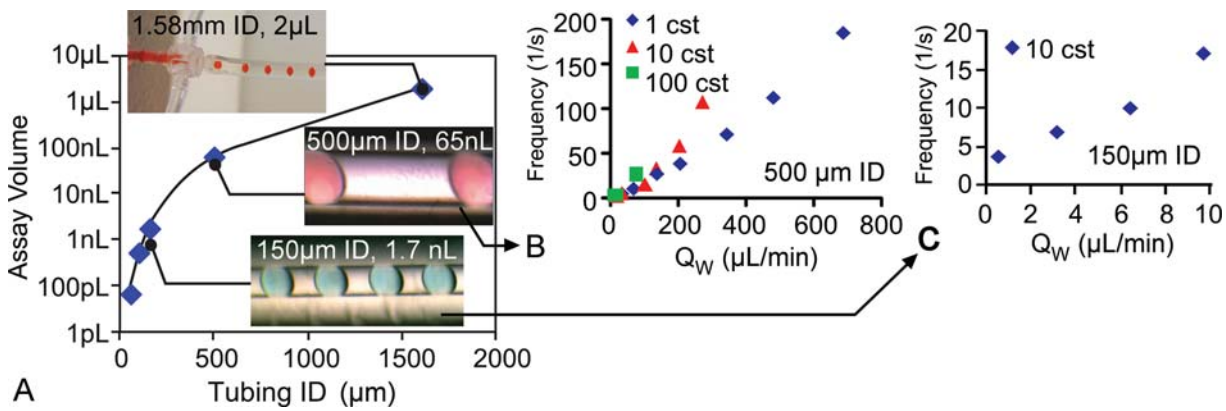

Fig. 4 (A) Scaling of droplet generation in different size tubing. Droplet frequency *versus* flow rate in (B) 500 μm tubing and (C) 150 μm tubing. See accompanying video in the ESI.‡

however, we focused on an isothermal condition, and an absence of surfactant.

Microfractionation

A C18 sep-pack cartridge (Discovery Sciences) was used to separate a mixture of dyes (FD&C Red No. 40, Blue No. 1, and Yellow No. 5). The dyes were dissolved in DI water and loaded into the column. After removing excess dye with DI water, the cartridge was connected to the drop generator, and eluted using 99% methanol at flow rates ranging from 100–1000 μl min^{-1}. Both the eluent and carrier fluid were provided by a syringe pump (KD Scientific). This experiment utilized the 1.5 mm tubing and fittings shown in Table 1.

In situ cell encapsulation and culture

C6 astrocytoma cells (ATCC) were grown in tissue culture flasks using F-12K medium supplemented with 10% horse serum, 2.5% FBS, and antibiotics. For testing, cells were trypsinized, counted using a hemocytometer, and resuspended in the 1% alginate solution. C6 cells were chosen for their phenotypic resemblance to native astrocytes. Typical flow rates were 60–300 μL min^{-1} on the oil syringe and 20–100 μL min^{-1} on the alginate and $BaCl_2$ syringes. In order to synchronize the coalescence of alginate and $BaCl_2$, identical flow-rates were used on both reagents. After the capsules were generated, they were collected in a beaker for subsequent viability analysis. The Live/Dead® viability/cytotoxicity assay (Invitrogen) was employed to determine cell viability post-encapsulation. The capsules containing the cells were rinsed three times using phosphate buffered saline (PBS) solution and then stained. The stain consisted of 200 μL of solution prepared from 5 mL Dulbecco's Modified Eagle Medium (DMEM) phenol-free culture media, 10 μL ethidium homodimer-1 (Etdh-1: detects dead cells) and 2.5 μL calcein AM (to detect live cells). Capsules were then incubated at 37 °C for 30 minutes. Fluorescence images were obtained using green (495–515 nm) and red (560–595 nm) emission filters. Images of different focal planes within the capsule were taken and then analyzed using an image processing software (ImageJ, National Institutes of Health). Percent surviving cells were determined by measuring the area of green signals divided by the area covered by the total number of cells (green + red fluorescence) at a given focal plane.

3. Results and discussion

3a. Components for drop generation, storage, and mixing

Droplet generation. The droplet generator consists of a commercially available cross junction where a stream of aqueous liquid is combined with two orthogonal streams of an immiscible carrier fluid.[4,24–28] Like other microfluidic drop generators, simulations and experimental data are consistent with the pressure-based pinchoff model described by Garstecki and Whitesides.[24,29] When a droplet fills the width of the junction, the flow of carrier fluid is temporarily blocked, resulting in a buildup of transverse pressure along the neck of the droplet which eventually pinches off the droplet (Fig. 2). A 1.5 mm ID cross-junction can form monodisperse droplets with volumes ~2 μL at a rate of 0.1–16 droplets per second. Smaller droplets (65 nL and 1.7 nL) can be generated by using 500 μm and 150 μm ID tubing, respectively (Fig. 3). Increasing the flow rate and carrier fluid viscosity increases drop generation frequency and reduces drop volume. The highest drop generation rate obtained is 190 drops per second in the 500 μm ID tubing using 1 cst silicone oil.

Analysis of drop generation. The behavior of hydrodynamic drop generators can be described by the capillary number $Ca = \mu_C V_C/\sigma$, where μ_C and V_C are the viscosity and velocity of the carrier fluid, respectively, and σ is the interfacial tension between the water and the carrier fluid.[29] In our experiments, we have used water and silicone oil with an interfacial tension of 30 mN m^{-1}.[21,22] The viscosity of the silicone oil ranges from 1 to 1000 cst, and experimental fluid velocity ranges from 0.1 to 100 mm s^{-1}. Consequently, the experiments span a wide range of Ca, and we observe a corresponding range in behavior.

When the Ca is small ($Ca < 0.002$), as is the case with most microfluidic drop generators,[25] drop formation is in the squeezing regime.[24] Here, the size of the droplet is independent of the capillary number and is determined instead by the size of the channel and the ratio Q_O/Q_W. Squeezing formation is observed in all tubing sizes when using low viscosity oil (1 and 10 cst). It is identified by the linear trend between drop frequency (f_d) and water flow rate (Q_W) (Fig. 2C, 4B and 4C). Given that $Q_W = f_d V_d$, a linear trend between Q_W and f_d implies that the droplet volume V_d is fixed. The squeezing regime is the most desirable region of drop generation, due to its linearity, and can be achieved by using low viscosity (1 and 10 cst) carrier fluid.

As Ca is increased (higher viscosity and/or flow rate), drop generation transitions from the squeezing to the dripping regime. In this regime, the drop volume is dependent on both the flow rate and the viscosity ratio between the water and the carrier fluid.[29] A CFD simulation (Fig. 5) qualitatively compares drop generation at 1 and 100 cst at a fixed flow rate. The high viscosity carrier fluid encounters more fluidic resistance between the droplet and the wall, which results in a faster pinch-off and smaller droplets. Increasing the flow rate also decreases the drop size. The characteristic nonlinearity of the dripping regime is observed in the frequency plot when using 1.5 mm tubing with high viscosity oil

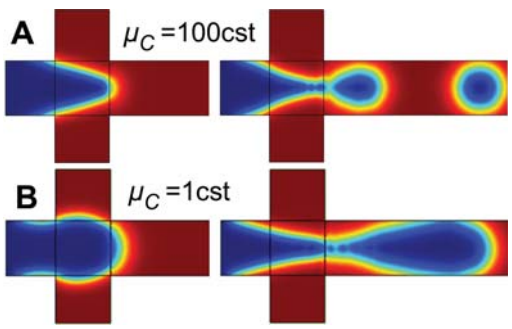

Fig. 5 Effect of carrier fluid viscosity on drop generation. The simulation shows drop generation in a 1.5 mm junction with identical velocities (14 mm s^{-1} water and 20 mm s^{-1} oil) but different viscosities of the carrier fluid. (A) 100 cst carrier fluid and (B) 1 cst carrier fluid.

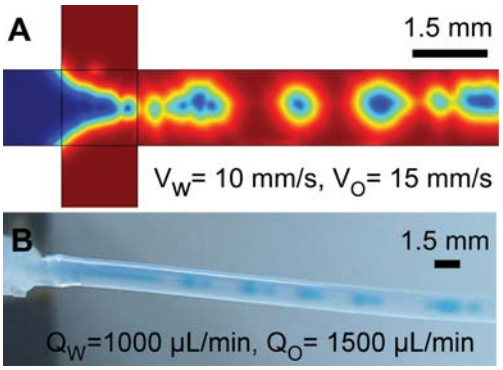

Fig. 6 Jet formation at high viscosity and flow rate. (A) 2D CFD simulation of jet breakup with 1 cst water and 1000 cst carrier fluid at the flow velocities shown. (B) Jet breakup with the same fluids and with the flow rates shown.

(100 and 1000 cst) and flow rates greater than 100 μL min^{-1} (Fig. 2C).

When *Ca* is increased even further (*Ca* > 0.2), jetting is observed (Fig. 6). Simulations and experiments qualitatively show jet formation and breakup resulting in polydisperse droplets. We have observed jetting in only one of our experiments which utilized the largest size tubing (1.5 mm), highest viscosity carrier fluid (1000 cst), and the highest flow rate (1000 μL min^{-1}). To avoid jetting, lower viscosity carrier fluids should be used at high flow rates.

Stability and repeatability of drop generation and storage. A robust droplet screening system must be able to generate and store large libraries of monodisperse droplets in a repeatable manner. Furthermore, when surfactants are not used, droplets must remain physically separated from one another to prevent merging. The stability of drop generation is quantified using the coefficient of variation (COV). The COV plot (Fig. 7) shows the

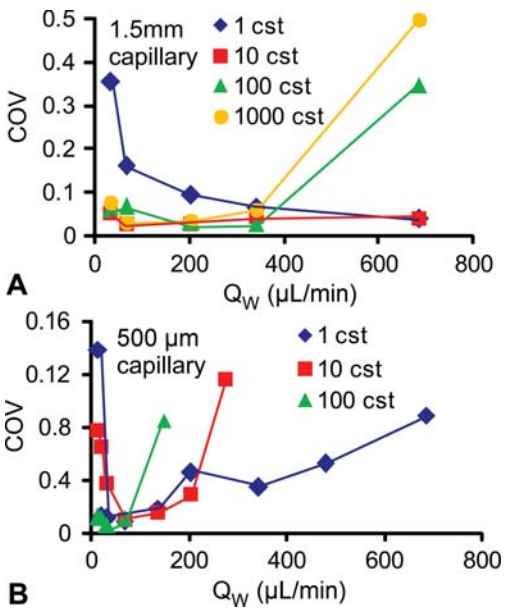

Fig. 7 Stability of drop generation. Coefficient of variation (COV) *versus* flow rate and viscosity for (A) 1.5 mm ID tubing and (B) 500 μm ID tubing.

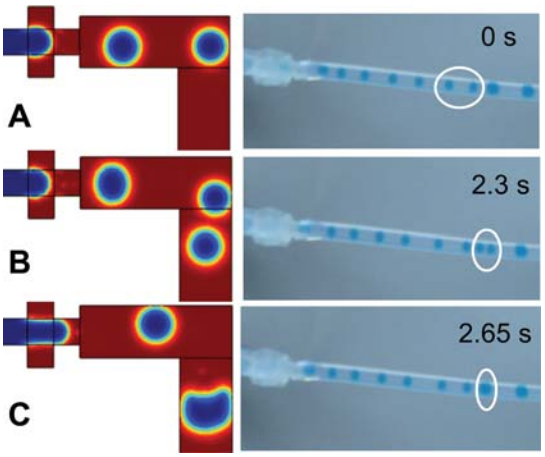

Fig. 8 Model for (undesirable) merging between adjacent drops. The left column shows simulations, in which a gravity condition is applied to model the effects of a tilted tubing. The right column shows experiments in a 1.5 mm ID capillaries placed at a 15 degree angle.

effect of flow rate and viscosity on the stability of drop formation. The combination of a high viscosity fluid and a high flow rate leads to a large COV because the system begins to transition into the drop jetting regime. It also generates a large back-pressure which leads to instability in the syringe pump. Conversely, when a low viscosity carrier fluid is used at low flow rates, gravitational forces can cause undesirable merging between adjacent drops (Fig. 8). As illustrated by the 2D simulation, aqueous drops in a less dense carrier fluid experience a negative buoyant force upon reaching a bend or tilt in the channel. If the viscosity of the carrier fluid is small, the oil separating two droplets drains through the space between the droplet and the wall, and the two adjacent drops merge. Overall, as a general rule of thumb, we conclude that high viscosity carrier fluids are better suited for low flow rates, while lower viscosity fluids are better suited for high flow rates. We have found that 10 cst silicone oil provides repeatable results over the range of flow rates we have tested.

Drop storage. Having determined the optimal range of conditions for drop generation over a range of tubing diameters and flow rates, it is then feasible to create large libraries of droplets in a repeatable manner (Fig. 9). The library can be compactly stored by wrapping a flexible capillary tube around a spool. The argument behind this approach is scalability. Although droplets can be stored at a high density on a PDMS microchip, the relatively small footprint of PDMS chips can make it difficult to store large libraries in a single file. Capillary tubing, on the other hand, can be purchased in long lengths for a few dollars per metre. Based on a 50/50 ratio of water to carrier fluid, a 1.5 mm ID capillary can store 333 droplets per metre, and a 150 μm capillary can store up to 3300 droplets per metre. Commercially available fused silica and PEEK tubing with 25 μm ID can provide up to 20 000 droplets per metre. In the last decade, large scale high throughput screening campaigns often involved libraries with over a million compounds. More recently, however, the HTS industry has shifted towards smaller, more focused libraries containing thousands of compounds.[30] For

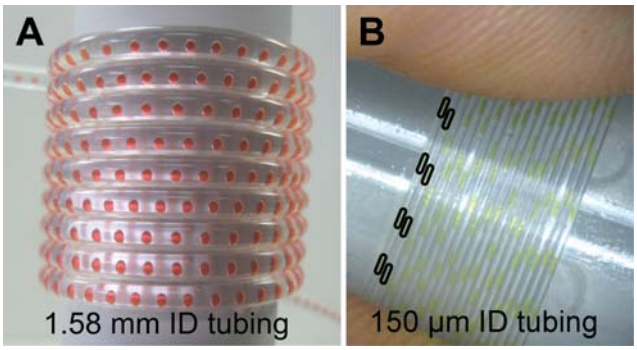

Fig. 9 Flexible capillary tubing wrapped around a spool allows large droplet libraries to be stored and transported in a compact format. (A) 2 μL droplets in 1.58 mm ID (1/16″) Teflon tubing and (B) 5 nL droplets in 150 μm ID Teflon tubing. See accompanying video in the ESI.‡

these and other areas (such as proteomics), the current approach can be an economical alternative to microplates which can reduce reagent consumption and eliminate the need for laboratory robotic pipettes.

Inline optical detectors. For optical interrogation of droplets, we demonstrate modular flow-through absorbance detectors using LEDs, fiber optics, and photodetectors at a cost of <$10.[31] As shown in Fig. 3A, a droplet passing by the detector causes a corresponding decrease in the photodetector signal which is exponentially related to the droplet concentration. LED light sources are generally economical, consume low power, are available over a wide range of wavelengths, and offer the possibility of electronic modulation for pulsed or lock-in detection schemes.[32–34] The primary issue in the design of the fiber optic absorbance detector is the placement of the fibers. Without the benefit of light focusing optics used in traditional detection systems, light loss does occur, but the loss is manageable if the fibers are axially aligned and placed close to one another. For example, the detector for 1.5 mm tubing utilizes 1 mm polymer optical fibers separated by 1.6 mm. At this gap, the light loss is 30–40%, which can be compensated by increasing the intensity of the light source. In the detectors for 500 and 150 μm ID tubing, the optical fibers are generally smaller, but they can be placed closer to one another, resulting in similar efficiency.

Although the sensitivity of fiber optic absorbance detectors is well below what is offered by confocal fluorescence, absorbance detectors can provide remarkably high performance when absorbance detection is needed. A previous report of an LED-based fiber-optic absorbance detectors showed that with carefully aligned fibers and differential detection methods, it is possible to achieve baseline noise levels better than commercial absorbance systems, with sensitivity in the range of micro-absorbance units.[35] In addition, the detectors can provide bandwidths in the range of 100s of MHz for high speed sensing. Due to the low cost, multiple detection modules can be added inline for comparative detection or for multi-wavelength measurements. Comparative detection is useful for assaying the droplet before and after adding the target reagent (Fig. 11), and multi-wavelength measurements can yield 2D scatter plots for identifying droplet populations, similar to flow cytometry[31] (Fig. 12). The width of the peaks (corresponding to droplet volume) and interpeak spacing (droplet period) can also be statistically tabulated, as described earlier in this report.

Mixing components. A key aspect of a droplet-based screening system is the ability to serially mix the target reagent with each droplet in the screening library. Mixing can be accomplished *via* a tee-junction.[2,4] A train of droplets is fed into one input of the junction, while a stream of the target reagent is fed into the second input. The addition of the target reagent to each droplet occurs in a 4 step process (Fig. 10). (i) *Attachment*: as the droplet enters the tee-junction, surface forces wick the interface to that of the target reagent. In the absence of stabilizing surfactants, the wicking process occurs spontaneously. (ii) *Mixing*: as the drop passes through the junction, it is 'coated' with the target reagent. The plug size increases due to the added fluid. (iii) *Necking*: the transverse pressure exerted on the droplet by the carrier fluid

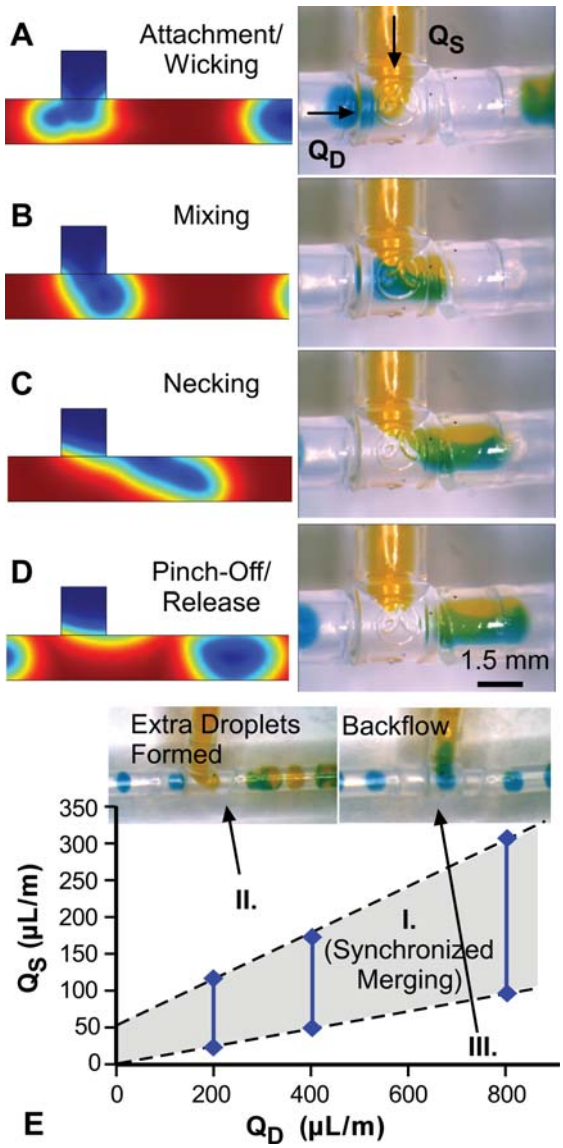

Fig. 10 Drop mixing using a tee-junction. (A–D) Simulation and experimental results showing the 4 steps of drop merging (see text for details). (E) Optimal conditions for synchronized drop merging. See accompanying video in the ESI.‡

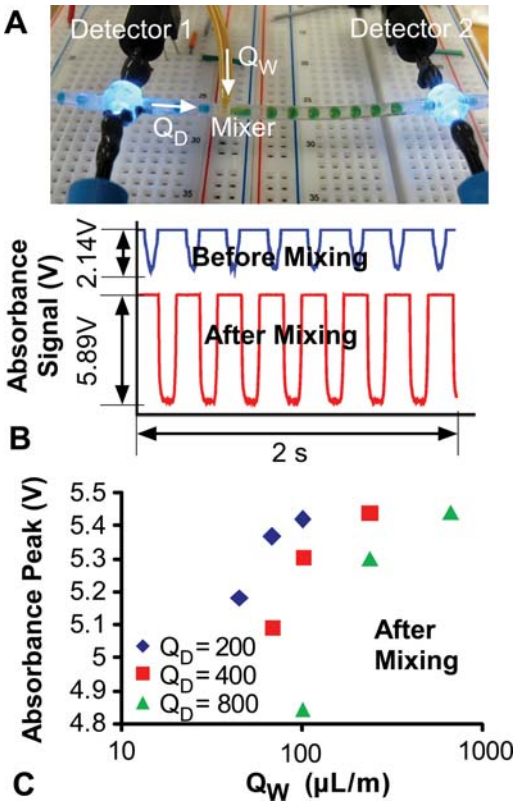

Fig. 11 *Mix and read assay*. (A) Experimental setup, showing assembly of the two detectors and a mixing junction. The upstream drop generator is not shown. (B) Photodetector signals obtained before and after mixing. (C) Amplitude of the absorbance peaks after mixing. See accompanying video in the ESI.‡

causes it to thin at the junction. (iv) *Pinch-off/release*: eventually, the mixed droplet pinches off and is released into the microchannel. Under the proper operating conditions, a fixed amount of target reagent is added to each droplet, and the process is self-synchronized. When synchronized, the volume of reagent added to each droplet is proportional to the flow rate of the stream Q_S. For each droplet flow rate Q_D, there is a corresponding range of compatible Q_S for which synchronous merging will occur (Fig. 10E, region I). If Q_S is too high, extra droplets of the target reagent are injected into the droplet train (region II). If Q_S is too low, the fluids from the droplet train backflow into the reagent stream (region III).

3b. Combining components to perform droplet-based assays

This section illustrates 3 useful protocols in droplet-based fluidics where the required system can be assembled from the basic components described above.

Example 1: "mix and read" assay. The simplest and most common type of assay used in HTS is the "mix and read" assay, where a collection of compounds is mixed to a single target reagent, and the results are optically interrogated.[36] Fig. 11 shows how the modular components described above can be combined to perform a mix and read assay in a droplet format similar to that proposed by Song *et al.*[2] Two absorbance detection modules ($\lambda = 470$ nm) are placed before and after the mixing junction to provide a comparative measurement. The low cost of the detection modules makes it feasible to include multiple modules, and the entire system can be assembled on an electronic breadboard for fast prototyping. The cost of the fluidic and detection components is <$20, and the assembly time is <10 minutes. In the mixing assay, the composite flow rate of the droplet train (Q_D) is fixed, and the flow rate of the aqueous stream (Q_S) is chosen to maintain synchronized merging (region I, Fig. 10E). The mixing junction serially combines blue-dyed (FD&C Blue No. 1, Allura Blue) droplets with yellow dye (FD&C Yellow #5, tartrazine) at the mixing junction. The absorbance of

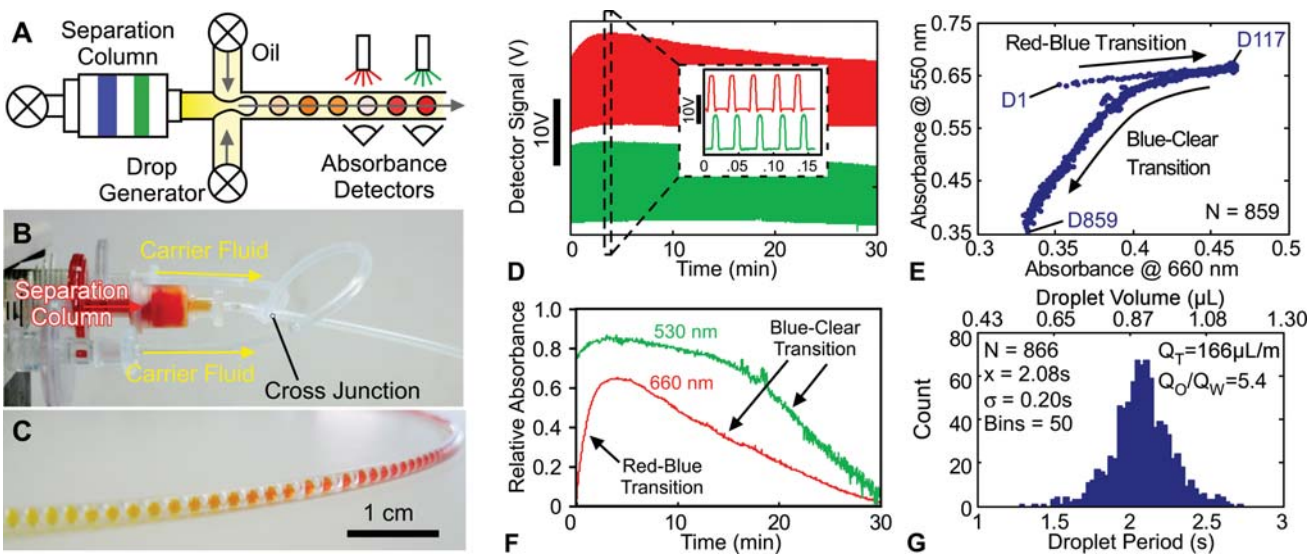

Fig. 12 *Microfractionation in droplets*. (A) System schematic, which includes a separation cartridge, drop generator, and absorbance detectors. (B) Experimental setup. (C) Library of drops of organic dyes obtained using μFD. *Characterization of μFD library using dual fiber optic detectors*. A mixture of red and blue dyes fractionated using this process is characterized with dual 530 and 660 nm detectors. (D) Raw data. (E) After envelope detection, showing absorbance at both wavelengths. (F) 2D scatter map for identifying droplet composition. (G) Histogram of droplet volume and period.

tartrazine at 470 nm results in a large absorbance signal after mixing, along with an increase in the peak width due to a larger droplet volume (Fig. 11B). As expected, we observe an increase in the absorbance peak with increasing Q_S (Fig. 11C).

Example 2: microfractionation in droplets (μFD). One of the challenging problems in droplet-based screening is how to generate a heterogeneous (chemically distinct) set of compounds in droplet form. Past efforts[13,37] generated droplet trains containing titrations of 2–3 reagents, but there were no simple methods to generate a train of *n* compounds. Using modular components, we recently demonstrated a technique for generating libraries of chemical compounds in droplet form[31] by coupling modular drop generators to chromatography-based separation processes. A cross-junction drop generator is attached to the end of a chromatography column (Fig. 12). As separated compounds exit the column, they are encapsulated into droplets, providing permanent separation between the compounds. Microfractionation has also been demonstrated using commercial chromatography processes with microfluidic chips.[38,39] A similar technique employed capillary electrophoresis as the separation process.[40] The use of standard components and fittings for μFD alleviates interconnect issues and provides direct compatibility with existing chromatography equipment. The drop library generated using μFD is analyzed by two cascaded absorbance detection modules, one at 530 nm, and the other at 660 nm. The peaks generated in the absorbance signal represent a "digital sampling" of the chromatogram (Fig. 12D). The system records each peak's amplitude and width, which correspond to the droplet's concentration and size, respectively. Envelope detection can be used to reconstruct the traditional "analog" chromatogram (Fig. 12E). In addition, the discrete absorbance data at multiple wavelengths allow droplet populations to be plotted on a 2D scatter plot, similar to flow cytometry (Fig. 12F). The size and spacing between drops are also recorded and tabulated (Fig. 12G). Together, these analyses enable the μFD system to "fingerprint" the composition of each droplet in the library before it is used in a screening assay.

Example 3: *in situ* cell culture. While droplets are well suited for solution-based screening, cell-based screens are more problematic because eukaryotes typically require attachment to solid supports to maintain viability and function. Using microfluidic chips, cells can be encapsulated in hydrogel beads, which act as a pseudo-solid support.[10,41–43] Using the modular components, we have shown that combining a drop generator, a mixer, and storage tubing can be used to encapsulate cells in hydrogel beads and culture them *in situ*.[11] Eukaryotic cell encapsulation and culture are accomplished in 3 steps (Fig. 13). First, drops containing cells and alginate solution are generated using a cross-junction. Second, each liquid drop is combined with a Barium Chloride ($BaCl_2$) crosslinker at a tee-junction. The crosslinker polymerizes the alginate (with minimal swelling), creating hydrogel beads which provide a pseudo-solid support for cell attachment.[44] Finally, the cells are cultured *in situ* by placing the entire tubing directly inside a conventional cell incubator. Like PDMS, Teflon's high gas permeability allows for respiratory exchange.[45] Cells can therefore survive until the depletion of nutrients and buildup of waste products in the capsule leads to mortality.[7] In our experiments, Live/Dead staining shows that 80% of the cells are viable after 3 days in culture, and 40% after 9 days. Micrographs (Fig. 13C) show that cells proliferate throughout the drop. Using this approach, several thousand cell reactors can be simultaneously cultured, with high viability sufficient for drug screening and toxicity assays.

Evaluation and comparison with PDMS. Table 2 compares the modular approach described in this paper with traditional droplet devices fabricated in PDMS using soft lithography. With regard to performance, PDMS-based devices offer a >1 order of magnitude faster throughput in drop generation and merging, and can also handle smaller volumes. Due to the maximum size limitation in devices formed using soft lithography, the largest drop volume is typically limited to about 1 nL. The present approach can offer a wider range of sizes due to the wide range of tubing ID available.

With regard to material properties, Teflon capillaries can provide some advantages in drop-based fluidics. For example, in

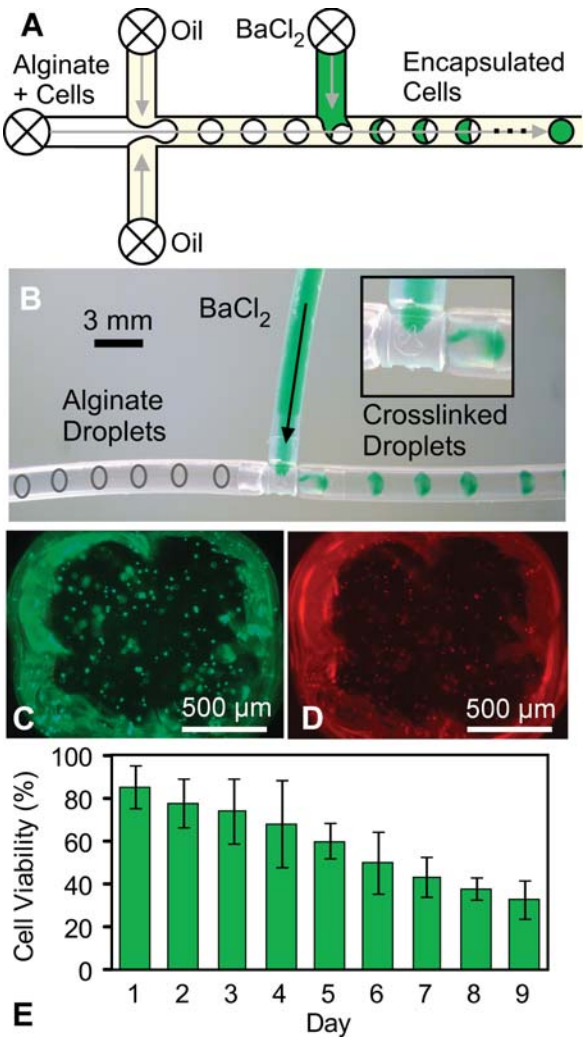

Fig. 13 *Cell encapsulation and in situ culture.* (A) Schematic of setup, which includes a drop generator and a mixing junction. (B) Operation of device. (C and D) Live/Dead staining of alginate capsules, used for measuring cell viability. (E) Cell viability over 9 days.

Table 2 Comparison of PDMS-based droplet microfluidic devices and the modular systems described in this paper

	PDMS/soft lithography	Modular using Teflon tubing (PTFE)
Water contact angle	109° native, 30° after O_2 Plasma[46]	110° Native, 170° after O_2 plasma[47]
Drop volume	1 pL to 1 nL[a]	65 pL to 2 μL
Drop generation rate	2000 drops per second[52]	200 drops per second
Merging rates	100 drops per second (electrocoalescence[53])	10 drops per second (T junction)
Detection	Microscope objectives	Fiber optic modules
Compatible carrier fluids	Compatible with a range of solvents; incompatible with silicone oil,[25] pentane, xylenes[b]	Inert to most chemicals
Optical properties	Transparent	Translucent
Gas permeable	Yes	Yes
Fabrication	Soft lithography (hours)[49]	Hand assembled from commercial parts (minutes)
Complex geometries	Straightforward	Difficult, often impossible
Interconnect	Friction fittings, bonded nanoports[54]	Commercially available barb, compression fittings
Maximum pressure	Up to 100 psi[50]	>5000 psi

[a] Limited by maximum size of PDMS channel. [b] For a list of compatible/incompatible solvents, see ref. 48.

droplet-based protein crystallization, native PDMS does not support plug formation because detergent solutions wet the walls, but Teflon capillaries are sufficient when used with fluorinated carrier fluids.[13] Both Teflon and PDMS have similar contact angles in their native state (~110°); however, after oxygen plasma treatment required for bonding, PDMS becomes hydrophilic (~30°).[46] Plasma treatment is not required with tubing; nonetheless, it is interesting to note that Teflon becomes more hydrophobic (~170°) after plasma treatment.[47] Another challenge with PDMS based devices is that several solvents cause PDMS to swell.[48] This is particularly problematic in droplet-based fluidics because many organic solvents serve as carrier fluids. Teflon is chemically inert, and is stable in a wider range of carrier fluids. For example, our experiments utilized silicone oil, which is known to cause swelling in PDMS,[25] but is compatible with Teflon tubing.

With regard to optical detection, PDMS is transparent, allowing trans-illumination and optical interrogation through the walls of the chip. Teflon is generally translucent, which limits visualization only to thin-walled tubing at a reduced resolution. For this reason, we utilize fiber optic detection modules in which the waveguides are inserted through the walls of the tubing. An alternative is to use fused silica tubing, which can provide transparent detection windows throughout the UV and visible wavelengths. When used for chemical separation and μFD, PDMS can support electroosmotic flow (EOF) when treated with oxygen plasma.[49] Teflon tubing cannot but other tubing (such as fused silica) can be used when specific surface charge is needed. In addition, the modular systems can be easily integrated with existing equipment for CE and chromatography as described earlier. When used for cell culture, both PDMS and Teflon provide high gas permeability which enables cells to be cultured *in situ*.

Fluidic interconnect is often a challenge in PDMS based devices, and is commonly the source of most leaks. Standard friction fittings (made by coring PDMS) support pressures up to 100 psi.[50] By comparison, modular fittings (generally compression type) can provide up to 5000 psi or higher. We have observed no leakage issues in our experiments.

Last is the tradeoff of complexity *versus* ease of fabrication. A major strength of PDMS-based devices is the level of integration and complexity possible only through lithographic fabrication.[51] The modular approach can only be used for simple systems, but they can be assembled in minutes rather than hours. The overall theme of this work is to illustrate that the two approaches are complementary, and both are important in the researcher's toolkit.

Conclusion

This paper reports on the use of modular, commercially available components to build droplet-based analysis systems. Drops can be generated at rates up to 200 drops per second, and merged at rates up to 10 drops per second. Although the throughput falls short of the highest performance PDMS drop generators, it is sufficient for most screening assays. In addition, it can provide a number of benefits to users in the screening community, including a wide range of assay volumes, scalable storage and transport, compatibility with a wide range of carrier fluids, simplified interconnect, and compatibility with existing laboratory infrastructure. For the research community, a modular approach can save time when prototyping new concepts in droplet-based screening systems. In the examples shown, the system modularity allowed for quick results without designing custom microfluidic chips. This, along with low-cost and widespread availability, suggests a useful and complementary approach to droplet-based fluidics.

References

1 A. Huebner, S. Sharma, M. Srisa-Art, F. Hollfelder, J. B. Edel and A. J. deMello, Microdroplets: a sea of applications? *Lab Chip*, 2008, **8**, 1244–1254.
2 H. Song, D. L. Chen and R. F. Ismagilov, Reactions in droplets in microfluidic channels, *Angew. Chem., Int. Ed.*, 2006, **45**, 7336.
3 S. Teh, R. Lin, L. Hung and A. P. Lee, Droplet microfluidics, *Lab Chip*, 2008, **8**, 198–220.
4 H. Song, J. D. Tice and R. F. Ismagilov, A microfluidic system for controlling reaction networks in time, *Angew. Chem., Int. Ed.*, 2003, **42**, 768.
5 J. Wölcke and D. Ullmann, Miniaturized HTS technologies–uHTS, *Drug Discovery Today*, 2001, **6**, 637–646.
6 E. Brouzes, M. Medkova, N. Savenelli, D. Marran, M. Twardowski, J. B. Hutchison, J. M. Rothberg, D. R. Link, N. Perrimon and M. L. Samuels, Droplet microfluidic technology for single-cell high-throughput screening, *Proc. Natl. Acad. Sci. U. S. A.*, 2009, **106**, 14195–14200.
7 J. Clausell-Tormos, D. Lieber, J. C. Baret, A. El-Harrak, O. J. Miller, L. Frenz, J. Blouwolff, K. J. Humphry, S. Köster and H. Duan, Droplet-based microfluidic platforms for the encapsulation and screening of mammalian cells and multicellular organisms, *Chem. Biol.*, 2008, **15**, 427–437.
8 S. Köster, F. E. Angile, H. Duan, J. J. Agresti, A. Wintner, C. Schmitz, A. C. Rowat, C. A. Merten, D. Pisignano and A. D. Griffiths, Drop-based microfluidic devices for encapsulation of single cells, *Lab Chip*, 2008, **8**, 1110–1115.

9 C. H. J. Schmitz, A. C. Rowat, S. Köster and D. A. Weitz, Dropspots: a picoliter array in a microfluidic device, *Lab Chip*, 2009, **9**, 44–49.
10 C. H. Choi, J. H. Jung, Y. W. Rhee, D. P. Kim, S. E. Shim and C. S. Lee, Generation of monodisperse alginate microbeads and *in situ* encapsulation of cell in microfluidic device, *Biomed. Microdevices*, 2007, **9**, 855–862.
11 V. Trivedi, E. Ereifej, A. Doshi, P. Sehgal, P. J. VandeVord and A. S. Basu, Microfluidic encapsulation of cells in alginate capsules for high throughput screening, *Conf. Proc. IEEE Eng. Med. Biol. Soc.*, 2009, 7037–7040.
12 L. Li, D. Mustafi, Q. Fu, V. Tereshko, D. L. Chen, J. D. Tice and R. F. Ismagilov, Nanoliter microfluidic hybrid method for simultaneous screening and optimization validated with crystallization of membrane proteins, *Proc. Natl. Acad. Sci. U. S. A.*, 2006, **103**, 19243.
13 B. Zheng, L. S. Roach and R. F. Ismagilov, Screening of protein crystallization conditions on a microfluidic chip using nanoliter-size droplets, *J. Am. Chem. Soc.*, 2003, **125**, 11170–11171.
14 L. Mazutis, J. C. Baret, P. Treacy, Y. Skhiri, A. F. Araghi, M. Ryckelynck, V. Taly and A. D. Griffiths, Multi-step microfluidic droplet processing: kinetic analysis of an *in vitro* translated enzyme, *Lab Chip*, 2009, **9**, 2902–2908.
15 D. S. Tawfik and A. D. Griffiths, Man-made cell-like compartments for molecular evolution, *Nat. Biotechnol.*, 1998, **16**, 652–656.
16 O. J. Miller, K. Bernath, J. J. Agresti, G. Amitai, B. T. Kelly, E. Mastrobattista, V. Taly, S. Magdassi, D. S. Tawfik and A. D. Griffiths, Directed evolution by *in vitro* compartmentalization, *Nat. Methods*, 2006, **3**, 561.
17 D. Snakenborg, M. Brivio and J. P. Kutter, Reconfigurable Modular System for Microfluidic Applications, *Proc. Micro Total Analysis Systems, Jeju, Korea*, 2009, pp. 1671–1673.
18 M. Rhee and M. A. Burns, Microfluidic assembly blocks, *Lab Chip*, 2008, **8**, 1365–1373.
19 K. A. Shaikh, K. S. Ryu, E. D. Goluch, J. Nam, J. Liu, C. S. Thaxton, T. N. Chiesl, A. E. Barron, Y. Lu, C. A. Mirkin and C. Liu, A modular microfluidic architecture for integrated biochemical analysis, *Proc. Natl. Acad. Sci. U. S. A.*, 2005, **102**, 9745–9750.
20 P. Grodzinski, J. Yang, R. H. Liu and M. D. Ward, A modular microfluidic system for cell pre-concentration and genetic sample preparation, *Biomed. Microdevices*, 2003, **5**, 303–310.
21 H. Mousa and T. G. M. van de Ven, Stability of water-in-oil emulsions in simple shear flow 2. The efforts of additives on the orthokinetic coalescence efficiency, *Colloids Surf.*, 1991, **60**, 39–51.
22 C. Wetterqvist, D. Wong, R. Williams, T. Stappler, E. Herbert and S. Freeburn, Tamponade efficiency of perfluorohexyloctane and silicone oil solutions in a model eye chamber, *Br. J. Ophthalmol.*, 2004, **88**, 692.
23 Z. Jiao, N. T. Nguyen and X. Huang, Thermocapillary actuation, *J. Micromech. Microeng.*, 2007, **17**, 1843–1852.
24 P. Garstecki, M. J. Fuerstman, H. A. Stone and G. M. Whitesides, Formation of droplets and bubbles in a microfluidic T-junction—scaling and mechanism of break-up, *Lab Chip*, 2006, **6**, 437–446.
25 S. L. Anna, N. Bontoux and H. A. Stone, Formation of dispersions using "flow focusing" in microchannels, *Appl. Phys. Lett.*, 2003, **82**, 364–366.
26 P. B. Umbanhowar, V. Prasad and D. A. Weitz, Monodisperse emulsion generation *via* drop break off in a coflowing stream, *Langmuir*, 2000, **16**, 347–351.
27 T. Thorsen, R. W. Roberts, F. H. Arnold and S. R. Quake, Dynamic pattern formation in a vesicle-generating microfluidic device, *Phys. Rev. Lett.*, 2001, **86**, 4163–4166.
28 T. Ward, M. Faivre, M. Abkarian and H. A. Stone, Microfluidic flow focusing: drop size and scaling in pressure *versus* flow-rate-driven pumping, *Electrophoresis*, 2005, **26**, 3716–3724.
29 M. De Menech, P. Garstecki, F. Jousse and H. A. Stone, Transition from squeezing to dripping in a microfluidic T-shaped junction, *J. Fluid Mech.*, 2008, **595**, 141–161.
30 K. H. Bleicher, H. J. Bohm, K. Muller and A. I. Alanine, Hit and lead generation: beyond high-throughput screening, *Nat. Rev. Drug Discovery*, 2003, **2**, 369–378.
31 A. Doshi, V. Trivedi, P. Sehgal and A. S. Basu, Digital Chromatography and the Formation of Heterogeneous droplet Libraries using Microfractionation in Droplets (μFD), *Proc. Micro Total Analysis Systems (MicroTAS)*, 2009.
32 Y. Suzuki, H. Hori, M. Iwatsuki and T. Yamane, A four-wavelength channel absorbance detector with a light emitting diode-fiber optics assembly for simplifying the flow-injection analysis system, *Anal. Sci.*, 2003, **19**, 1025–1028.
33 P. K. Dasgupta, I. Eom, K. J. Morris and J. Li, Light emitting diode-based detectors: absorbance, fluorescence and spectroelectrochemical measurements in a planar flow-through cell, *Anal. Chim. Acta*, 2003, **500**, 337–364.
34 L. Novak, P. Neuzil, J. Pipper, Y. Zhang and S. Lee, An integrated fluorescence detection system for lab-on-a-chip applications, *Lab Chip*, 2007, **7**, 27–29.
35 P. A. G. Butler, B. Mills and P. C. Hauser, Capillary electrophoresis detector using a light emitting diode and optical fibres, *Analyst*, 1997, **122**, 949–953.
36 S. A. Sundberg, High-throughput and ultra-high-throughput screening: solution-and cell-based approaches, *Curr. Opin. Biotechnol.*, 2000, **11**, 47–53.
37 N. Damean, L. F. Olguin, F. Hollfelder, C. Abell and W. T. S. Huck, Simultaneous measurement of reactions in microdroplets filled by concentration gradients, *Lab Chip*, 2009, **9**, 1707–1713.
38 A. B. Theberge, G. Whyte and W. T. S. Huck, Generation of picoliter droplets with defined contents and concentration gradients from the separation of chemical mixtures, *Anal. Chem.*, 2010, **82**, 3449–3453.
39 X. Z. Niu, B. Zhang, R. T. Marszalek, O. Ces, J. B. Edel, D. R. Klug and A. J. deMello, Droplet-based compartmentalization of chemically separated components in two-dimensional separations, *Chem. Commun.*, 2009, 6159–6161.
40 J. Edgar, G. Milne, Y. Zhao, C. Pabbati, D. Lim and D. Chiu, Compartmentalization of chemically separated components into droplets, *Angew. Chem., Int. Ed.*, 2009, **48**, 2719–2722.
41 W. Tan and S. Takeuchi, Monodisperse alginate hydrogel microbeads for cell encapsulation, *Adv. Mater.*, 2007, **19**, 2696–2701.
42 K. Liu, H. Ding, J. Liu, Y. Chen and X. Zhao, Shape-controlled production of biodegradable calcium alginate gel microparticles using a novel microfluidic device, *Langmuir*, 2006, **22**, 9453–9457.
43 V. L. Workman, S. B. Dunnett, P. Kille and D. D. Palmer, On-chip alginate microencapsulation of functional cells, *Macromol. Rapid Commun.*, 2008, **29**, 165–170.
44 R. C. de Guzman, E. S. Ereifej, K. M. Broadrick, R. A. Rogers and P. J. VandeVord, Alginate-matrigel microencapsulated Schwann cells for inducible secretion of glial cell line derived neurotrophic factor, *J. Microencapsulation*, 2008, **25**, 487–498.
45 L. K. Massey, *Permeability properties of plastics and elastomers: a guide to packaging and barrier materials*, William Andrew, 2003, pp. 102–108.
46 J. C. McDonald, M. L. Chabinyc, S. J. Metallo, J. R. Anderson, A. D. Stroock and G. M. Whitesides, Prototyping of microfluidic devices in poly(dimethylsiloxane) using solid-object printing, *Anal. Chem.*, 2002, **74**, 1537–1545.
47 M. Morra, E. Occhiello and F. Garbassi, Contact angle hysteresis in oxygen plasma treated poly(tetrafluoroethylene), *Langmuir*, 1989, **5**, 872–876.
48 J. N. Lee, C. Park and G. M. Whitesides, Solvent compatibility of poly (dimethylsiloxane)-based microfluidic devices, *Anal. Chem.*, 2003, **75**, 6544–6554.
49 D. C. Duffy, J. C. McDonald, O. J. A. Schueller and G. M. Whitesides, Rapid prototyping of microfluidic systems in poly(dimethylsiloxane), *Anal. Chem.*, 1998, **70**, 4974–4984.
50 A. M. Christensen, D. A. Chang-Yen and B. K. Gale, Characterization of interconnects used in PDMS microfluidic systems, *J. Micromech. Microeng.*, 2005, **15**, 928–934.
51 T. Thorsen, S. J. Maerkl and S. R. Quake, Microfluidic large-scale integration, *Science*, 2002, **298**, 580–584.
52 J. J. Agresti, E. Antipov, A. R. Abate, K. Ahn, A. C. Rowat, J. Baret, M. Marquez, A. M. Klibanov, A. D. Griffiths and D. A. Weitz, Ultrahigh-throughput screening in drop-based microfluidics for directed evolution, *Proc. Natl. Acad. Sci. U. S. A.*, 2010, **107**, 4004–4009.
53 K. Ahn, J. Agresti, H. Chong, M. Marquez and D. A. Weitz, Electrocoalescence of drops synchronized by size-dependent flow in microfluidic channels, *Appl. Phys. Lett.*, 2006, **88**, 264105.
54 C. Koch, J. Ingle and V. Remcho, Lab on a Chip, Chips & Tips: bonding Upchurch® nanoPorts to PDMS, 2008, http://www.rsc.org/Publishing/Journals/lc/Chips_and_Tips/nanoport_bonding.asp.

